

Confined Pt and CoFe₂O₄ Nanoparticles in a Mesoporous Core/Shell Silica Microsphere and Their Catalytic Activity

Donghyeon Kang, Min-Sik Eum, Byeongno Lee, Tae-Sung Bae,[†]
Kyu Reon Lee, Heung Bin Lim,[‡] and Nam Hwi Hur^{*}

Department of Chemistry, Sogang University, Seoul 121-742, Korea. *E-mail: nhhur@sogang.ac.kr

[†]Korea Basic Science Institute, Jeonju 561-765, Korea

[‡]Department of Chemistry, Dankook University, Gyeonggi-do 448-701, Korea

Received July 10, 2011, Accepted August 22, 2011

Confined Pt and CoFe₂O₄ nanoparticles (NPs) in a mesoporous core/shell silica microsphere, Pt-CoFe₂O₄@meso-SiO₂, were prepared using a bi-functional linker molecule. A large number of Pt NPs in Pt-CoFe₂O₄@meso-SiO₂, ranging from 5 to 8 nm, are embedded into the shell and some of them are in close contact with CoFe₂O₄ NPs. The hydrogenation of cyclohexene over the Pt-CoFe₂O₄@meso-SiO₂ microsphere at 25 °C and 1 atm of H₂ yields cyclohexane as a major product. In addition, it gives oxygenated products. Control experiments with ¹⁸O-labelled water and acetone suggest that surface-bound oxygen atoms in CoFe₂O₄ are associated with the formation of the oxygenated products. This oxidation reaction is operative only if CoFe₂O₄ and Pt NPs are in close contact. The Pt-CoFe₂O₄@meso-SiO₂ catalyst is separated simply by a magnet, which can be re-used without affecting the catalytic efficiency.

Key Words : Magnetic nanoparticles, Core/Shell silica, Catalyst, Proximity effect

Introduction

Supported metal catalysts are typically composed of noble metal nanoparticles (NPs) immobilized on the surface of various oxide supports.¹⁻⁶ Catalytic activity of the supported catalyst is dependent on not only the size of metal NPs but also the metal-support interaction.⁷⁻¹³ Strong metal-support interaction in which metals are anchored on active transition metal oxides such as TiO₂,¹⁴⁻¹⁹ CeO₂,²⁰⁻²⁴ and Fe₂O₃,²⁵⁻²⁷ provides high activity for several reactions such as hydrogenation,²⁸⁻³⁰ CO oxidation,³¹⁻³⁵ and water-gas shift reaction.³⁶⁻³⁹ The underlying origin of the metal-support interaction and the promotional role of the active oxide supports in enhancing the catalytic activity and selectivity have thus been extensively studied.⁴⁰⁻⁴⁷ Relatively, little is known about direct interfacial interaction between metal NPs and support oxide NPs in a confined geometry. It would thus be interesting to study noble metal and active metal oxide with a well-defined nanostructure, which will render an important clue to elucidate the proximal metal-oxide interaction in nanometer scale⁴⁸⁻⁵⁰ and will also give a chance to develop a hybrid catalytic system on the basis of metal and oxide.⁵¹⁻⁵⁵

Gold NPs supported on metal oxides are known to be highly efficient for the oxidation reactions under relatively mild conditions.^{56,57} In particular, Hughes *et al.* reported that supported Au catalysts are very effective for the oxidation of cyclohexene in the presence of molecular oxidant although they require temperatures above 80 °C.⁵⁸ More recently, Enache *et al.* revealed that Au-Pd catalysts supported on TiO₂ provide exceptionally high turn-over frequencies for the oxidation of alcohols in which the addition of gold to palladium increases the selectivity.⁵⁹ These studies have tri-

ggered new interest in the development of oxidation catalysts on the basis of active metals supported on various solid oxides.

In the present work, we report the synthesis of Pt and CoFe₂O₄ NPs encapsulated within mesopores of the core/shell silica microsphere, hereafter Pt-CoFe₂O₄@meso-SiO₂, and their catalytic activity toward the hydrogenation of cyclohexene. An interesting feature is that encapsulated Pt and CoFe₂O₄ NPs not only show the facile conversion of cyclohexene to cyclohexane but also exhibit excellent synergy in the oxidation of cyclohexene. Our studies provide an important evidence that Pt NPs contacted with CoFe₂O₄ NPs are able to oxidize cyclohexene in liquid medium under the ambient conditions, which has not been found in the Pt-based catalysts. On the basis of catalytic experiments with ¹⁸O-labelled species as well as surface studies by electron microscopy, we have found that the interfacial interaction between the Pt and CoFe₂O₄ NPs results in the unusual oxidation of cyclohexene. The CoFe₂O₄ NPs not only provide a magnetic component for recyclable support⁶⁰⁻⁶³ but also play a significant role to promote the oxidation reaction if they are in proximal distance with the Pt NPs.

Experimental

Synthesis of Pt-CoFe₂O₄@meso-SiO₂ Microsphere. The superparamagnetic mesoporous microspheres, CoFe₂O₄@meso-SiO₂, were prepared by incorporating CoFe₂O₄ components into the mesoporous shell of the SiO₂ spheres, which were used as supports for embedding platinum NPs. Detailed procedures are described in our previous report.⁶⁴ A 100 mL flask was charged with CoFe₂O₄@meso-SiO₂ (0.150 g) and

ethanol (10 mL). The solution was sonicated for 1 h to disperse the CoFe₂O₄@meso-SiO₂ microspheres without agglomeration, to which 0.1 mL of 3-aminopropyltrimethoxy-silane (APTMS) was added drop by drop. The reaction mixture was then vigorously stirred for 3 h to bind APTMS molecules on the surfaces of the CoFe₂O₄@meso-SiO₂ microspheres. The functionalized CoFe₂O₄@meso-SiO₂ microspheres were purified by centrifuging the microspheres, discarding the supernatant, and re-dispersing them in ethanol. For the Pt loading into the microspheres, 0.010 g of K₂PtCl₄ (98+%, Aldrich) in 10 mL of distilled water was added to the functionalized CoFe₂O₄@meso-SiO₂ microspheres in 10 mL of ethanol, which was stirred for 6 h. The reaction yields a dark brown solution, indicating the deposition of Pt NPs on CoFe₂O₄@meso-SiO₂. After centrifuging the solution, the supernatant was discarded and the microspheres were washed with ethanol twice. The Pt-loaded CoFe₂O₄@meso-SiO₂ microsphere, denoted as Pt-CoFe₂O₄@meso-SiO₂, was dried in an oven at 80 °C, which was then annealed at 300 and 500 °C under argon atmosphere to ensure the strong adhesion of Pt NPs on the mesoporous silica surface.

Preparation of Pt@meso-SiO₂ Microsphere. Pt NPs were immobilized on the same mesoporous silica microspheres in a similar way to prepare the CoFe₂O₄@meso-SiO₂ microsphere. All the procedures are virtually identical except the mesoporous silica spheres were used as supports instead of using the CoFe₂O₄@meso-SiO₂ microspheres. The resulting Pt-anchored silica spheres, denoted as Pt@meso-SiO₂, were also sintered at 300 and 500 °C under argon atmosphere to ensure the strong adhesion of Pt NPs on the silica surface.

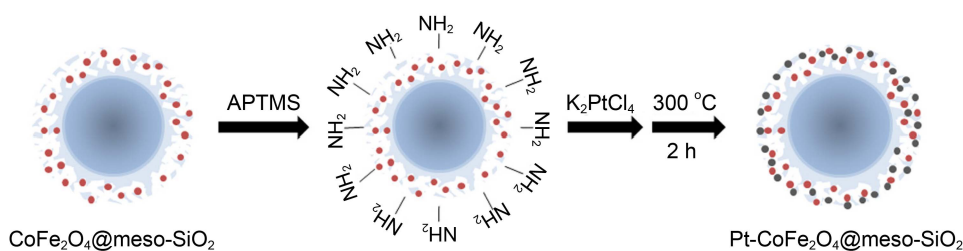
Catalytic Hydrogenation Reactions with Pt-CoFe₂O₄@meso-SiO₂, Pt@meso-SiO₂, and CoFe₂O₄@meso-SiO₂. A 10 mL round bottom flask with side arms was charged with the Pt-CoFe₂O₄@meso-SiO₂ catalyst (0.0050 g). To the flask were added 4 mL of acetone (GC grade, ≥ 99.5%, Aldrich) and 0.1 mL of cyclohexene (GC grade, 99.99%, Fluka) by using a syringe. The reaction mixture was allowed to react at room temperature for 10 h under a hydrogen atmosphere, in which the pressure was maintained using a balloon filled with hydrogen gas. The products were analyzed by gas chromatography (GC), which was compared with authentic samples. A permanent magnet was used to separate the Pt-CoFe₂O₄@meso-SiO₂ catalyst from the reaction mixture. The used catalyst was washed several times with ethanol and completely dried at room temperature prior to using again. For comparison, some of the used catalysts were annealed at 300 °C in air. Catalysis runs using them were carried out under the same conditions. The products were analyzed by GC in a similar manner. All the other control experiments, including the catalytic reactions with Pt@meso-SiO₂ and CoFe₂O₄@meso-SiO₂, were also performed under the same conditions.

Preparation of ¹⁸O-labelled Acetone. A 10 mL of round bottom flask was charged with 2 mL of ¹⁸O-labelled water (Cambridge Isotope Laboratories, Inc., 97% of ¹⁸O), 5 mL of acetone (Aldrich, GC grade, ≥ 99.5%), and 0.1 mL of sulfuric acid (Aldrich, 99.999%). The mixture was stirred vigorously

for 6 h. After stirring, ¹⁸O-labelled acetone was separated from the mixture by using cold trap under vacuum. About 4.4 mL of acetone was collected. The ratio of ¹⁸O-labelled acetone to ¹⁶O acetone was 1.0:1.7 on the basis of the GC-mass analysis.

Catalytic Hydrogenation Reactions using ¹⁸O-labelled Acetone and ¹⁸O-labelled Water. A 10 mL of round bottom flask filled with 5 mg of the Pt-CoFe₂O₄@meso-SiO₂ catalyst was vacuum-dried at 300 °C for 6 h to remove water completely in the flask and the catalyst. After cooling the flask, 4 mL of ¹⁸O-labelled acetone as prepared and 0.1 mL of cyclohexene (Fluka, GC grade, 99.99%) were added into the flask. The reaction mixture was allowed to react at room temperature for 10 h under the hydrogen atmosphere, in which the pressure was maintained using a balloon filled with the hydrogen gas. For the catalytic experiment with ¹⁸O-labelled water, a 10 mL of round bottom flask filled with 5 mg of the Pt-CoFe₂O₄@meso-SiO₂ catalyst was dried in a similar manner. After cooling the flask, 4 mL of acetone (Aldrich, GC grade, ≥ 99.5%), 0.1 mL of cyclohexene (Fluka, GC grade, 99.99%), and 0.1 mL of ¹⁸O-labelled water (Cambridge Isotope Laboratories, Inc., 97% of ¹⁸O) were added into the flask. The reaction mixture was allowed to react at room temperature for 10 h under the hydrogen atmosphere, in which the pressure was also maintained using a balloon filled with hydrogen gas. The products were analyzed by a GC-mass to confirm the existence of ¹⁸O in the oxidized products. A permanent magnet was used to separate the Pt-CoFe₂O₄@meso-SiO₂ catalyst from the reaction mixture.

Characterizations and Analysis. Powder X-ray diffraction patterns were recorded with a Rigaku DMAX 2500 diffractometer (Cu K α) operating at 40 kV and 150 mA. High resolution scanning electron microscope (HR-SEM) analyses were carried out using a Hitachi s-5500. Samples for HR-SEM were prepared by dropping the diluted sample in ethanol on a grid. Transmission electron microscope (TEM) analyses were carried out on a JEOL JEM-2100F. Samples were also subjected to chemical microanalysis with an Oxford Instruments INCA TEM 300 system for energy dispersive X-ray (EDX) analysis. Specimens for TEM examination were prepared by dispersing the finely-ground powder in high purity ethanol and then allowing a drop of the suspension to evaporate on a 400 mesh carbon-coated grid. Another quantitative analysis of Pt-CoFe₂O₄@meso-SiO₂ was determined by inductively coupled plasma-mass spectrometry. About 5 mg of the Pt-CoFe₂O₄@meso-SiO₂ sample was weighed and transferred into a vessel for microwave acid digestion. Then, 2 mL of HF, 2 mL of H₂SO₄ and 5 mL of HNO₃ were added into the vessel, followed by the programmed procedure for the digestion. The digested solution was cooled to room temperature, which was delivered into a 100 mL volumetric flask. After the solution was properly diluted, contents of Pt, Si, Fe, and Co in the solution were determined by ICP-MS. Relative weight percentage of Pt is 5.23%. GC analyses were carried out using a YoungLin Model system with a flame induced detector using an HP-5 capillary column. In ¹⁸O labelling experiments, products diluted in mesitylene



Scheme 1. Reaction scheme for employment of Pt NPs into a CoFe_2O_4 @meso- SiO_2 microsphere. Red and gray dots denote CoFe_2O_4 and Pt NPs, respectively.

were analyzed by HP 5890/5972 GC-mass spectroscopy using a HP-5 capillary column.

Results and Discussion

Synthesis and Characterization of Pt- CoFe_2O_4 @meso- SiO_2 NPs. Our approach to confine Pt and CoFe_2O_4 NPs within pores is based on mesoporous core/shell silica (meso- SiO_2) microspheres that have a well-defined nanostructure.⁶⁵ The CoFe_2O_4 @meso- SiO_2 spheres with a diameter of about 500 nm were initially prepared by incorporating magnetic components (CoFe_2O_4) into porous silica shells according to our previous report.⁶⁴ As shown in Scheme 1, a CoFe_2O_4 @meso- SiO_2 microsphere is treated with a bi-functional APTMS (3-aminopropyl-trimethoxysilane) molecule. In this process, neither heating nor reflux was needed. Stirring is sufficient to make amine-functionalized CoFe_2O_4 @meso- SiO_2 microspheres because silane groups of APTMS molecules easily combine with hydroxyl residues on the surface of the silica spheres. Terminal silane groups are attached to a surface of CoFe_2O_4 @meso- SiO_2 , leaving behind amine functionalized magnetic spheres. The free terminal amine groups on CoFe_2O_4 @meso- SiO_2 can then serve as nucleation sites for the growth of Pt NPs. The reduction of K_2PtCl_4 with ethanol yields Pt NPs, which are readily immobilized on the surfaces of the functionalized CoFe_2O_4 @meso- SiO_2 microspheres by coordinating to the nitrogen of the amine groups. The resulting Pt-immobilized spheres, Pt- CoFe_2O_4 @meso- SiO_2 , are annealed at 300 and 500 °C to make Pt NPs crystalline as well as to bind Pt NPs on the silica surface strongly. In a similar way, Pt NPs are attached to the same mesoporous silica microspheres in which distinctive color change from white to gray is noticed, indicating that the Pt NPs are well incorporated into the SiO_2 microspheres.

The growth and size of Pt NPs on the amine-functionalized surface is very sensitive to the relative concentrations of ethanol and water. The optimization is accomplished using several mixtures of ethanol and water at different ratios. When the ethanol to water ratio is 1:3, individual Pt NPs are well separated and evenly distributed on the silica surface. Increasing the amount of ethanol, however, resulted in the formation of large Pt clusters, suggesting that facile reduction leads to the agglomeration of Pt NPs. In the presence of a mixture containing less than 10% of ethanol, on the other hand, the extremely sparse deposition of Pt NPs on a CoFe_2O_4 @meso- SiO_2 microsphere is observed, imply-

ing that the reduction is not properly operative because of low ethanol content.

Figure 1 shows powder X-ray diffraction (XRD) patterns for the Pt- CoFe_2O_4 @meso- SiO_2 microspheres annealed at 300 and 500 °C in Ar. Peaks corresponding to CoFe_2O_4 are clearly seen in both samples. The peak broadening is not severe so that all the peaks can be well indexed in a cubic lattice (space group: $Fd\bar{3}m$). Average grain sizes of CoFe_2O_4 for the 300 and 500 °C samples calculated by the Scherrer equation are 11.5 and 13.5 nm, respectively. Their grain sizes are not noticeably influenced by the post-annealing. The XRD peaks ascribed to Pt NPs, on the other hand, are very sensitive to the annealing temperature. Two distinctive but broad peaks that can be indexed with a cubic symmetry (space group: $Fm\bar{3}m$) of Pt are observed in the 500 °C sample whereas very broad peaks that are not easily distinguished from the noise peaks are observed in the 300 °C sample. This demonstrates that grain sizes of the 300 °C sample are extremely small. According to the Scherrer equation, average Pt sizes in the 300 and 500 °C samples are calculated to be 3.4 and 5.2 nm, respectively.

TEM images of the Pt- CoFe_2O_4 @meso- SiO_2 spheres annealed at 300 and 500 °C are shown in Figure 2, revealing that the morphology of the parent silica sphere with a core/shell structure is not noticeably changed by post-heating. Even upon annealing the sample at 700 °C, the spherical

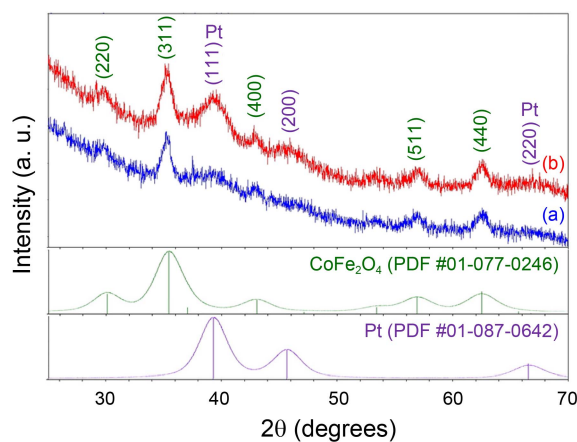


Figure 1. Powder XRD patterns for Pt- CoFe_2O_4 @meso- SiO_2 microspheres annealed at (a) 300 and (b) 500 °C. Below the XRD patterns simulated XRD patterns for cubic CoFe_2O_4 and Pt phases are shown respectively, in which particle sizes were considered. Vertical bars are literature reflections and relative intensities of the CoFe_2O_4 and Pt structures.

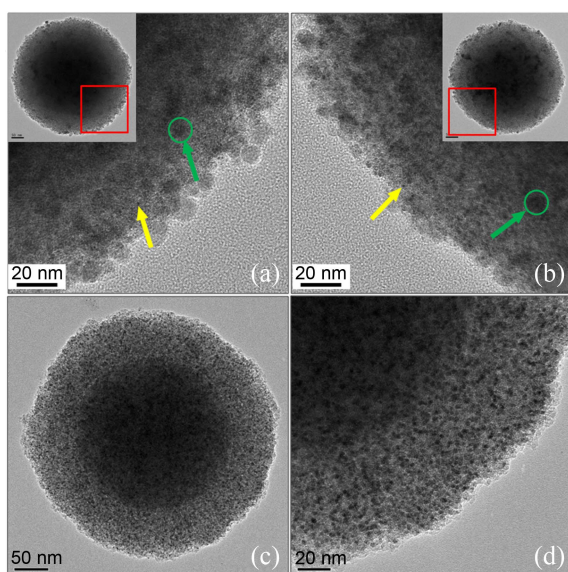


Figure 2. Overall TEM images of Pt-CoFe₂O₄@meso-SiO₂ microspheres annealed at (a) 300 and (b) 500 °C are shown in insets. High resolution TEM images correspond to red-lined square areas of the insets. Areas denoted as green circles indicate CoFe₂O₄ NPs embedded within mesoporous silica shells and small black dots pointed by yellow arrow represent Pt NPs. (c) Pt@meso-SiO₂ microspheres annealed at 500 °C and (d) its magnified image are shown.

core/shell shape of Pt-CoFe₂O₄@meso-SiO₂ was preserved and the Pt NPs were still embedded within the silica shell, implying high thermal stability of Pt NPs immobilized on the silica surface. As can be seen in the TEM images, Pt NPs (yellow arrows) are uniformly distributed in the pores within a silica shell, suggesting that this strategy to immobilize Pt NPs on the amine-functionalized silica surface by direct alcohol reduction can be an ideal method to strongly anchor metal NPs on the oxide surface. Figure 2(c) and (d) show TEM images of Pt-CoFe₂O₄@meso-SiO₂ spheres. Small Pt NPs with similar size are evenly anchored on the silica surface while relatively larger NPs corresponding to CoFe₂O₄ are rarely seen in the TEM images.

A careful comparison of the TEM images between the 300 and 500 °C samples reveals that the size of Pt NPs became slightly larger after heating at 500 °C, which is probably ascribed to the growth of Pt NPs at the Pt-SiO₂ interface. By heat treatment, the Pt NPs continue to grow and become highly crystalline while maintaining the surface morphology. It seems that post-heat treatment is of importance to not only increase size but also deposit Pt NPs uniformly on the silica surface. It is worth mentioning that Pt NPs do not show any deformation or agglomeration up to 500 °C. However, agglomeration of Pt NPs was observed in the annealed sample at temperatures above 700 °C, implying that Pt NPs slightly diffuse into the neighbouring Pt-CoFe₂O₄ phases through the mesoporous silica shell.

Figure 3 illustrates elemental distribution maps of Pt, Co, and Fe in the same region of a Pt-CoFe₂O₄@meso-SiO₂ microsphere, which were obtained using a TEM equipped

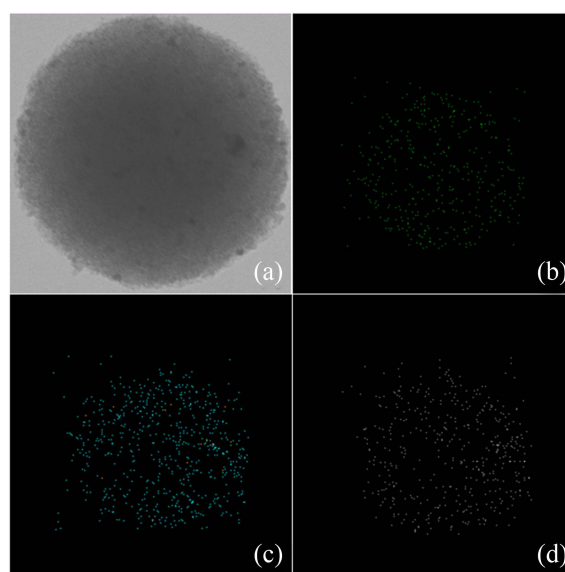


Figure 3. (a) High resolution TEM image of a Pt-CoFe₂O₄@meso-SiO₂ microsphere annealed at 300 °C. Elemental distribution maps of (b) Pt, (c) Fe, and (d) Co present in the microsphere, which are taken by energy-filtered TEM.

with an energy-dispersive X-ray (EDX) analyzer. We can see uniform distribution of the three elements in the sample, indicating that Pt and CoFe₂O₄ NPs are embedded within a silica shell without any agglomeration. As expected, Co and Fe appear in almost the same areas in a Pt-CoFe₂O₄@meso-SiO₂ microsphere, implying that binary oxides such as Co₃O₄ and Fe₃O₄ are less likely to be formed. Relative weight percentages of Pt, Co, and Fe incorporated in silica microspheres determined by an EDX analyzer are 5.73, 1.28, and 2.70, respectively. These weight percentages are close to those obtained from inductively coupled plasma mass spectrometry analysis. A SQUID magnetometer was also employed to evaluate the magnetic properties of parent CoFe₂O₄@meso-SiO₂ spheres, showing that superparamagnetic phases are present in the microspheres. Details on the magnetic properties were described in our previous paper.⁶⁴

High-resolution SEM images of a Pt-CoFe₂O₄@meso-SiO₂ microsphere annealed at 300 °C are shown in Figure 4, revealing that two types of NPs with different sizes and shapes appear to be immobilized on the surface. One group consists of many small spherical dots marked as yellow arrows, which are uniformly spread over the whole silica surface whose sizes are in the range of 3 to 5 nm. The dots are the most likely to be Pt NPs on the basis of XRD and elemental analysis data. The other is composed of relatively small numbers of large spherical dots, denoted as red dotted lines that appear to be issued out from silica mesopores. Their sizes are typically larger than 10 nm, which are probably ascribed to CoFe₂O₄ NPs. An important feature is that CoFe₂O₄ NPs are sparsely located in the silica surface and each CoFe₂O₄ dot is surrounded by several Pt NPs. Relative ratio of Pt and CoFe₂O₄ NPs and their locations turn out to be a very important factor to elucidate unusual oxidation products obtained from the hydrogenation reaction

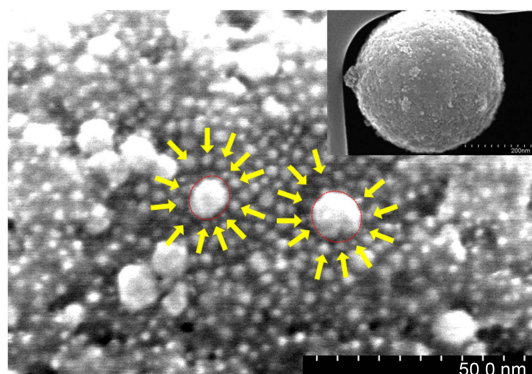
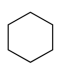
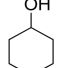
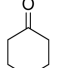


Figure 4. High resolution SEM images of a Pt-CoFe₂O₄@meso-SiO₂ microsphere annealed at 300 °C. The inset is an overall image of a Pt-CoFe₂O₄@meso-SiO₂ particle. Yellow arrows and red dotted circles denote Pt and CoFe₂O₄ NPs immobilized on a silica shell, respectively. A CoFe₂O₄ NP is surrounded by a number of Pt NPs.

of cyclohexene using the Pt-CoFe₂O₄@meso-SiO₂ microsphere, which will be discussed below.

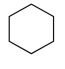
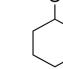
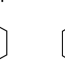
Catalytic Activities. Catalytic activity of the Pt-CoFe₂O₄@meso-SiO₂ microsphere was initially tested for cyclohexene hydrogenation because platinum is known to be an active catalyst for most hydrogenation reactions.⁶⁶⁻⁷⁰ The reactions were performed in acetone at 25 °C and 1 atm of H₂, where the gas pressure was maintained with a hydrogen-filled balloon. Complete conversion of cyclohexene is accomplished within 10 h and the main product is cyclohexane. An interesting feature in the hydrogenation reaction over the Pt-CoFe₂O₄@meso-SiO₂ microsphere is that oxygenated products such as cyclohexanol and cyclohexanone were also obtained under the hydrogen atmosphere. To elucidate the role of Pt and CoFe₂O₄ NPs, the same reaction was carried out with the Pt@meso-SiO₂ catalyst containing only Pt NPs in the mesoporous shell. As shown in Table 1, cyclohexene was completely converted to cyclohexane within 10 h and no oxygenated products were observed. These results clearly suggest that the Pt-CoFe₂O₄@meso-SiO₂ catalyst promotes the oxidation of cyclohexene even in the absence of molecular oxidants such as hydrogen peroxide and *t*-butyl hydroperoxide at ambient conditions. This

Table 1. Catalytic reactions of cyclohexene by Pt@meso-SiO₂ and Pt-CoFe₂O₄@meso-SiO₂ catalysts^a

Catalyst	Conversion ^b	Product selectivity ^c			Total Oxidation Product ^d
					
Pt@meso-SiO ₂	100	99.9	-	-	-
Pt-CoFe ₂ O ₄ @meso-SiO ₂	100	91.5	7.6	1.2	8.8

^aReaction conditions: catalyst, 5 mg; substrate (cyclohexene), 0.1 mL; solvent (acetone), 4 mL; atmosphere, 1 atm of H₂; time, 10 h; temperature, 25 °C. ^bDetermined by the ratio of remained cyclohexene. ^cDetermined by the integrations of GC peaks. ^dConversion multiplied by sum of oxidation products.

Table 2. Catalytic reactions of cyclohexene by Pt-CoFe₂O₄@meso-SiO₂ catalyst under different gas atmospheres^a

Gas ^b	Conversion ^d	Product selectivity ^e			Total Oxidation Product ^f
					
H ₂	100	91.5	7.6	1.2	8.8
O ₂	-	-	-	-	-
H ₂ /O ₂ ^c	41.7	97.2	2.1	0.6	1.1

^aReaction conditions: catalyst, Pt-CoFe₂O₄@meso-SiO₂, 5 mg; substrate (cyclohexene), 0.1 mL; solvent (acetone), 4 mL; time, 10 h; temperature, 25 °C. ^bGas atmosphere: 1 atm of each gas. ^cTwo gases were mixed with 1:1 volume ratio. ^dDetermined by the ratio of remained cyclohexene. ^eDetermined by the integrations of GC peaks. ^fConversion multiplied by sum of oxidation products.

hydrocarbon oxidation has not been observed in the Pt-based catalyst although Au and Pd NPs supported on various supports are found to be effective catalysts for the oxidation of alcohols in the presence of oxidants.^{58,59}

To understand this unexpected oxidation in the hydrogen atmosphere over the Pt-CoFe₂O₄@meso-SiO₂ catalyst, a wide range of control experiments using compositionally modified catalysts were performed under the same conditions. The hydrogenation reaction was done with the CoFe₂O₄@meso-SiO₂ microsphere to check the catalytic activity of CoFe₂O₄ NPs, which was almost insensitive to the hydrogenation reaction. Negligible amount of cyclohexene conversion was observed. This indicates that CoFe₂O₄ NPs alone cannot activate cyclohexene at ambient conditions. A subsequent experiment using the meso-SiO₂ microsphere revealed no catalytic activity toward the hydrogenation. All of the above results suggest that the hydrogenation reaction takes place solely over Pt NPs whereas the oxidation of cyclohexene takes place only when both Pt and CoFe₂O₄ NPs are in closely contact. As given in Table 2, the Pt-CoFe₂O₄@meso-SiO₂ catalyst yields oxygenated products only in the hydrogen atmosphere. Under the oxygen atmosphere, surprisingly, no conversion took place. This indicates that oxidation reactions are associated with hydrogen rather than oxygen.

The oxygenated products obtained from the hydrogenation reaction with the Pt-CoFe₂O₄@meso-SiO₂ catalyst evidently ensure the employment of oxygen in cyclohexene. To determine the origin of oxygen in the products, we initially performed the cyclohexene hydrogenation with the same Pt-CoFe₂O₄@meso-SiO₂ catalyst using ¹⁸O-labelled acetone. No discernible amount of ¹⁸O-labelled species, which was evaluated by mass spectrometry, was observed in the oxygenated products. Analogous experiment with ¹⁸O-labelled water was also carried out to check the possibility of water as the oxygen source. Little ¹⁸O species in the oxygenated products was also found, clearly showing that both acetone and water have less chance to provide oxygen in the oxygenated products.

Labelling studies suggest that surface oxygen in the supported oxide (CoFe₂O₄) is the likely source of oxygen. It has

been known that surface lattice oxygen located at coordinatively unsaturated sites readily incorporates into the substrates.^{71,72} Although the incorporation of oxygen from surface oxide into cyclohexene at ambient conditions in liquid medium is not clearly understood at this stage, a plausible explanation is that a spill-over of hydrogen from the Pt NPs to the surface oxide leads to the generation of reactive oxygen species or hydroxy ions.

To show the involvement of surface oxide in the oxidation of cyclohexene, we performed the same hydrogenation reactions with the Pt-CoFe₂O₄@meso-SiO₂ catalysts repeatedly, which might provide an important clue to elucidate whether surface oxides are involved in the formation of oxygenated products. In an initial set of experiments, the same hydrogenation reactions were performed with used catalysts in which the Pt-CoFe₂O₄@meso-SiO₂ catalysts were recovered by a magnet and were reused without any regeneration procedure. The catalytic reactions were carried out up to five times while maintaining previous reaction conditions (25 °C and 1 atm of H₂ in acetone). As shown in Figure 5, oxidation products were drastically decreased even after the first run. For comparison, we studied the same catalytic reactions with replenished Pt-CoFe₂O₄@meso-SiO₂ catalysts, in which the catalysts were prepared by annealing used Pt-CoFe₂O₄@meso-SiO₂ catalysts at 300 °C in air. Virtually identical amount of oxidation products were obtained from the hydrogenation reactions with replenished Pt-CoFe₂O₄@meso-SiO₂ catalysts, which is illustrated in Figure 5. The two experiments reveal that surface lattice oxygen atoms in CoFe₂O₄ are incorporated into the oxygenated products. As demonstrated in the previous experiments, the CoFe₂O₄ NPs do not play a role to catalyze the oxidation of cyclohexene. However, they are involved in the oxidation reaction when they are closely interacted with Pt NPs. It is thus reasonable to infer that the oxidation reaction is driven by both CoFe₂O₄ and Pt NPs. It has been known that mobility of surface oxygen in noble metal catalysts supported on solid oxides is accelerated by noble metals,⁷³ which can support the unusual oxidation of cyclohexene over Pt-CoFe₂O₄@meso-SiO₂.

To explore how Pt NPs interact with CoFe₂O₄ NPs within a mesoporous shell, we examined the surface morphology of the Pt-CoFe₂O₄@meso-SiO₂ catalyst thoroughly. Typical high-resolution SEM images of a Pt-CoFe₂O₄@meso-SiO₂ microsphere in Figure 6 support the idea of proximal inter-

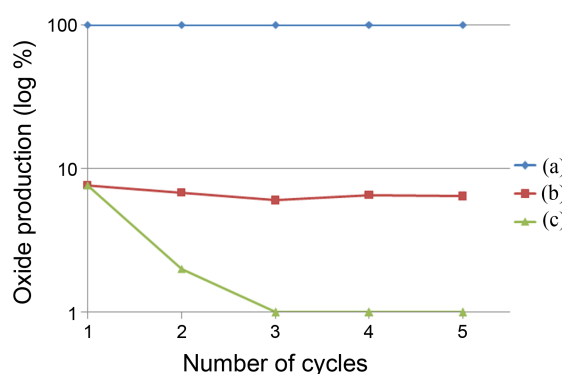


Figure 5. Percentages of oxidation products produced from the Pt-CoFe₂O₄@meso-SiO₂ catalysts as a function of catalytic cycle. (a) Percentage of total conversion is close to 100% for all the catalysts. Percentages of oxidation products using (b) the Pt-CoFe₂O₄@meso-SiO₂ catalyst refreshed in air at 300 °C and (c) the Pt-CoFe₂O₄@meso-SiO₂ catalyst without refreshment. All reactions were carried out in acetone at 25 °C and 1 atm of H₂.

action between CoFe₂O₄ and Pt NPs. As shown in the image of Figure 6(b), a large number of small Pt NPs are evenly distributed on the shell and large CoFe₂O₄ NPs are sparsely located. The CoFe₂O₄ NPs appear to be surrounded by several Pt NPs. The micro-structural images could provide an indirect evidence to understand the metal (Pt) – support (CoFe₂O₄) interaction in the catalytic reactions, suggesting that the hydrogenation reaction occurs solely on Pt NPs whereas the oxidation takes place over the contacted area between Pt and CoFe₂O₄ NPs.

In summary, we have synthesized the Pt-CoFe₂O₄@meso-SiO₂ catalyst in which both Pt and CoFe₂O₄ NPs are embedded within mesopores of the core/shell silica microsphere. We found that the Pt-CoFe₂O₄@meso-SiO₂ catalyst can oxidize cyclohexene in the absence of oxidant as well as convert readily cyclohexene to cyclohexane. A notable feature is that this oxidation occurs only if Pt NPs are in close contact with CoFe₂O₄ NPs. The surface bound oxygen in solid oxide plays a crucial role to generate the oxygenated products. This proximity-induced oxidation can be considered as the so-called strong-metal support interaction. The easy separation and reusability of the Pt-CoFe₂O₄@meso-SiO₂ catalyst is an additional prominent feature, which makes it a competitive catalyst for various industrial reactions and a wide range of organic transformations.

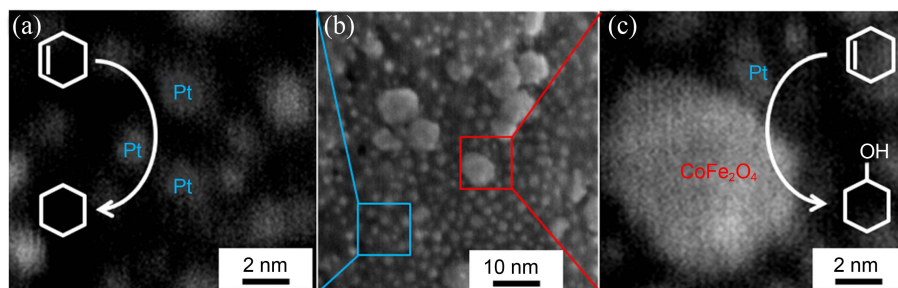


Figure 6. Enlarged high resolution SEM images of a Pt-CoFe₂O₄@meso-SiO₂ microsphere. The left and right panels are the expanded views of the blue and red square regions, respectively. Hydrogenation takes place over the Pt-rich region while oxidation occurs on the proximate region of Pt and CoFe₂O₄ NPs.

Acknowledgments. This study was supported by the Converging Research Center Program (2010K001050) and the Korea Center for Artificial Photosynthesis (KCAP) funded by the Ministry of Education, Science, and Technology through the National Research Foundation of Korea (NRF-2010-C1AAA001-2010-0028905). We also acknowledge the support of NRL (2010-0018937) and KETEP (2008-E-AP-HM-P-1-0000).

References

- Kim, Y.-W.; Kim, M.-J. *Bull. Korean Chem. Soc.* **2010**, *31*, 1368.
- Costi, R.; Saunders, A. E.; Banin, U. *Angew. Chem. Int. Ed.* **2010**, *49*, 4878.
- Ojeda, M.; Iglesia, E. *Angew. Chem. Int. Ed.* **2009**, *48*, 4800.
- Guo, S.; Dong, S.; Wang, E. *J. Phys. Chem. C* **2008**, *112*, 2389.
- Yoo, J. W.; Lee, S.-M.; Kim, H.-T.; El-Sayed, M. A. *Bull. Korean Chem. Soc.* **2004**, *25*, 843.
- Mallat, T.; Baiker, A. *Chem. Rev.* **2004**, *104*, 3037.
- Mager-Maury, C.; Bonnard, G.; Chizzallet, C.; Sautet, P.; Raybaud, P. *ChemCatChem* **2011**, *3*, 200.
- Kaden, W. E.; Wu, T.; Kunkel, W. A.; Anderson, S. L. *Science* **2009**, *326*, 826.
- Grybos, R.; Benco, L.; Bucko, T.; Hafner, J. *J. Chem. Phys.* **2009**, *130*, 104503/1.
- Weerachawanasak, P.; Praserttham, P.; Arai, M.; Panpranot, J. *J. Mol. Catal. A: Chem.* **2008**, *279*, 133.
- Turner, M.; Golovko, V. B.; Vaughan, O. P. H.; Abdulkin, P.; Berenguer-Murcia, A.; Tikhov, M. S.; Johnson, B. F. G.; Lambert, R. M. *Nature* **2008**, *454*, 981.
- Haruta, M. *Catal. Today* **1997**, *36*, 153.
- Tauster, S. J.; Fung, S. C.; Garten, R. L. *J. Am. Chem. Soc.* **1978**, *100*, 170.
- Panagiotopoulou, P.; Kondarides, D. I.; Verykios, X. E. *J. Phys. Chem. C* **2011**, *115*, 1220.
- Huang, H.; Leung, D. Y. C. *ACS Catal.* **2011**, *1*, 348.
- Huang, S.-Y.; Ganesan, P.; Park, S.; Popov, B. N. *J. Am. Chem. Soc.* **2009**, *131*, 13898.
- Lopez-Sanchez, J. A.; Lennon, D. *Appl. Catal., A* **2005**, *291*, 230.
- Li, Y.; Xu, B.; Fan, Y.; Feng, N.; Qiu, A.; He, J. M. J.; Yang, H.; Chen, Y. *J. Mol. Catal. A: Chem.* **2004**, *216*, 107.
- Sohn, J. R.; Lee, J. S. *Bull. Korean Chem. Soc.* **2003**, *24*, 159.
- Sharma, S.; Hegde, M. S. *J. Chem. Phys.* **2009**, *130*, 114706/1.
- Miedziak, P. J.; Tang, Z.; Davies, T. E.; Enache, D. I.; Bartley, J. K.; Carley, A. F.; Herzing, A. A.; Kiely, C. J.; Taylor, S. H.; Hutchings, G. J. *J. Mater. Chem.* **2009**, *19*, 8619.
- Azad, A.-M.; Duran, M. J.; McCoy, A. K.; Abraham, M. A. *Appl. Catal., A* **2007**, *332*, 225.
- Yeung, C. M. Y.; Yu, K. M. K.; Fu, Q. J.; Thompsett, D.; Petch, M. I.; Tsang, S. C. *J. Am. Chem. Soc.* **2005**, *127*, 18010.
- Roh, H.-S.; Jun, K.-W.; Baek, S.-C.; Park, S.-E. *Bull. Korean Chem. Soc.* **2002**, *23*, 799.
- Wong, K.; Zeng, Q. H.; Yu, A. B. *J. Phys. Chem. C* **2011**, *115*, 4656.
- Routray, K.; Zhou, W.; Kiely, C. J.; Wachs, I. E. *ACS Catal.* **2011**, *1*, 54.
- Herzing, A. A.; Kiely, C. J.; Carley, A. F.; Landon, P.; Hutchings, G. J. *Science* **2008**, *321*, 1331.
- Lee, J.-K.; Kim, D.-W.; Cheong, M.-S.; Lee, H.-J.; Cho, B.-W.; Kim, H.-S.; Mukherjee, D. *Bull. Korean Chem. Soc.* **2010**, *31*, 2195.
- Corma, A.; Serna, P. *Science* **2006**, *313*, 332.
- Chen, C.-S.; Chen, H.-W.; Cheng, W.-H. *Appl. Catal., A* **2003**, *248*, 117.
- Shon, J.-K.; Park, J.-N.; Hwang, S.-H.; Jin, M.; Moon, K.-Y.; Boo, J.-H.; Han, T.-H.; Kim, J.-M. *Bull. Korean Chem. Soc.* **2010**, *31*, 415.
- Santos, V. P.; Carabineiro, S. A. C.; Tavares, P. B.; Pereira, M. F. R.; Orfao, J. J. M.; Figueiredo, J. L. *Appl. Catal., B* **2010**, *99*, 198.
- Min, M.-K.; Kim, J.-H.; Kim, H.-S. *Bull. Korean Chem. Soc.* **2010**, *31*, 151.
- Jiang, H.-L.; Liu, B.; Akita, T.; Haruta, M.; Sakurai, H.; Xu, Q. *J. Am. Chem. Soc.* **2009**, *131*, 11302.
- Haruta, M.; Kobayashi, T.; Sano, H.; Yamada, N. *Chem. Lett.* **1987**, *16*, 405.
- Rodriguez, J. A.; Graciani, J.; Evans, J.; Park, J. B.; Yang, F.; Stacchiola, D.; Senanayake, S. D.; Ma, S.; Pérez, M.; Liu, P.; Sanz, J. F.; Hrbek, J. *Angew. Chem. Int. Ed.* **2009**, *48*, 8047.
- Burch, R. *PCCP* **2006**, *8*, 5483.
- Byun, I.-S.; Choi, O.-L.; Choi, J.-G.; Lee, S.-H. *Bull. Korean Chem. Soc.* **2002**, *23*, 1513.
- Sakurai, H.; Ueda, A.; Kobayashi, T.; Haruta, M. *Chem. Commun.* **1997**, *271*.
- Hoxha, F.; Schmidt, E.; Mallat, T.; Schimmoeller, B.; Pratsinis, S. E.; Baiker, A. *J. Catal.* **2011**, *278*, 94.
- Zope, B. N.; Hibbitts, D. D.; Neurock, M.; Davis, R. J. *Science* **2010**, *330*, 74.
- Zhai, Y.; Pierre, D.; Si, R.; Deng, W.; Ferrin, P.; Nilekar, A. U.; Peng, G.; Herron, J. A.; Bell, D. C.; Saltsburg, H.; Mavrikakis, M.; Flytzani-Stephanopoulos, M. *Science* **2010**, *329*, 1633.
- Liu, H.; Jiang, T.; Han, B.; Liang, S.; Zhou, Y. *Science* **2009**, *326*, 1250.
- Casaletto, M. P.; Longo, A.; Martorana, A.; Prestianni, A.; Venezia, A. M. *Surf. Interface Anal.* **2006**, *38*, 215.
- Alfredsson, M.; Catlow, C. R. A. *PCCP* **2002**, *4*, 6100.
- Venezia, A. M.; Rossi, A.; Duca, D.; Martorana, A.; Deganello, G. *Appl. Catal., A* **1995**, *125*, 113.
- Sankar, G.; Rao, C. N. R.; Rayment, T. *J. Mater. Chem.* **1991**, *1*, 299.
- Xu, L.; Ma, Y.; Zhang, Y.; Jiang, Z.; Huang, W. *J. Am. Chem. Soc.* **2009**, *131*, 16366.
- Wang, C.; Daimon, H.; Sun, S. *Nano Lett.* **2009**, *9*, 1493.
- Kim, Y. N.; Lee, E. K.; Lee, Y. B.; Shim, H.; Hur, N. H.; Kim, W. S. *J. Am. Chem. Soc.* **2004**, *126*, 8672.
- Bonanni, S.; Ait-Mansour, K.; Brune, H.; Harbich, W. *ACS Catal.* **2011**, *1*, 385.
- Fu, Q.; Li, W.-X.; Yao, Y.; Liu, H.; Su, H.-Y.; Ma, D.; Gu, X.-K.; Chen, L.; Wang, Z.; Zhang, H.; Wang, B.; Bao, X. *Science* **2010**, *328*, 1141.
- González, J. C.; Hernández, J. C.; López-Haro, M.; del Río, E.; Delgado, J. J.; Hungria, A. B.; Trasobares, S.; Bernal, S.; Midgley, P. A.; Calvino, J. J. *Angew. Chem. Int. Ed.* **2009**, *48*, 5313.
- Carrier, X.; Marceau, E.; Carabineiro, H.; Rodriguez-Gonzalez, V.; Che, M. *PCCP* **2009**, *11*, 7527.
- Rodriguez, J. A.; Hrbek, J. *Acc. Chem. Res.* **1999**, *32*, 719.
- Dapurkar, S. E.; Shervani, Z.; Yokoyama, T.; Ikushima, Y.; Kawanami, H. *Catal. Lett.* **2009**, *130*, 42.
- Lucchesi, C.; Inasaki, T.; Miyamura, H.; Matsubara, R.; Kobayashi, S. *Adv. Synth. Catal.* **2008**, *350*, 1996.
- Hughes, M. D.; Xu, Y.-J.; Jenkins, P.; McMorn, P.; Landon, P.; Enache, D. I.; Carley, A. F.; Attard, G. A.; Hutchings, G. J.; King, F.; Stitt, E. H.; Johnston, P.; Griffin, K.; Kiely, C. J. *Nature* **2005**, *437*, 1132.
- Enache, D. I.; Edwards, J. K.; Landon, P.; Solsona-Espriu, B.; Carley, A. F.; Herzing, A. A.; Watanabe, M.; Kiely, C. J.; Knight, D. W.; Hutchings, G. J. *Science* **2006**, *311*, 362.
- Polshettiwar, V.; Varma, R. S. *Org. Biomol. Chem.* **2009**, *7*, 37.
- Campelo, J. M.; Luna, D.; Luque, R.; Marinas, J. M.; Romero, A. A. *ChemSusChem* **2009**, *2*, 18.
- Jeong, U.; Teng, X.; Wang, Y.; Yang, H.; Xia, Y. *Adv. Mater.* **2007**, *19*, 33.
- Yoon, T.-J.; Lee, W.; Oh, Y.-S.; Lee, J.-K. *New J. Chem.* **2003**, *27*, 227.
- Lee, K. R.; Kim, S.; Kang, D. H.; Lee, J. I.; Lee, Y. J.; Kim, W. S.;

- Cho, D.-H.; Lim, H. B.; Kim, J.; Hur, N. H. *Chem. Mater.* **2008**, *20*, 6738.
65. Büchel, G.; Unger, K. K.; Matsumoto, A.; Tsutsumi, K. *Adv. Mater.* **1998**, *10*, 1036.
66. Pasricha, R.; Bala, T.; Biradar, A. V.; Umbarkar, S.; Sastry, M. *Small* **2009**, *5*, 1467.
67. Olivas, A.; Jerdev, D. I.; Koel, B. E. *J. Catal.* **2004**, *222*, 285.
68. Concepcion, P.; Corma, A.; Silvestre-Albero, J.; Franco, V.; Chane-Ching, J. Y. *J. Am. Chem. Soc.* **2004**, *126*, 5523.
69. Ammari, F.; Lamotte, J.; Touroude, R. *J. Catal.* **2004**, *221*, 32.
70. von Arx, M.; Mallat, T.; Baiker, A. *J. Mol. Catal. A: Chem.* **1999**, *148*, 275.
71. Kwak, J. H.; Hu, J.; Mei, D.; Yi, C.-W.; Kim, D. H.; Peden, C. H. F.; Allard, L. F.; Szanyi, J. *Science* **2009**, *325*, 1670.
72. Tsuji, H.; Hattori, H. *ChemPhysChem* **2004**, *5*, 733.
73. Martin, D.; Duprez, D. *J. Phys. Chem. B* **1997**, *101*, 4428.
-